Fig. 5. Cephalon of an *Asteropyge* sp. (Lehmann, 1934) (× 4.5).

of soft parts, especially in the trilobites examined so far.

The famous *Phacops* sp. (cover photograph) described in 1930 by Broili (*4*; *7*, figure 57E, p. O 81) shows details that cannot be made visible by mechanical preparation. Now observable on the x-ray photographs are the intestinal tract as well as the appendages with the gill filaments and other details, the most surprising of them being light guides leading from the facets of the eyes of the *Phacops* nearly to the center of the head (Fig. 3). There seems to be a significant difference between the facet eye structure of the horseshoe crab (*Limulus polyphemus*) and the eye of *Phacops* [earlier and recent work on the lens structure of trilobites did not reveal such details (*8–10*)]. The eyes of other *Phacops* species show similar structures (Fig. 4). In no case were interconnections found between the single fibers as described and explained in their function by Miller *et al.* (*11*) and by Ratliff *et al.* (*12*). From these observations it must be concluded that the filamentary structures are probably real light guides and not nerve bundles (as in the *Limulus* eye) guiding the light from the cornea over a rather long distance to the receptors in the vicinity of the brain. Contrary to the structure of the *Phacops* eyes, that of another trilobite, *Asteropyge* sp., described by Lehmann (*5*; *7*, figure 57A, p. O 81), shows more similarities to normal facet eyes of the insects (Fig. 5). Details of the eyes of this specimen were first revealed on an x-ray photograph by Lehmann (*5*), but he hesitated to explain what he saw as it seemed incredible to him that "the nerve bundles were going at an angle of about 45° backwards to a place where the ganglion of the lower throat is located" (*13*, figures 47 and 1). New radiographs of the specimen confirmed these earlier observations.

My experience with prepared and unprepared fossils of Devonian slates suggests that no mechanical preparation should be done prior to a thorough x-ray examination, in order to avoid the destruction of important fine details. In the course of the survey made in the last 2 years, several completely unknown Devonian fossils have been discovered.

WILHELM STUERMER
Burgbergstrasse 20,
8520 Erlangen, West Germany

References and Notes

1. R. G. Johnson and E. S. Richardson, Jr., *Science* **159**, 526 (1968).
2. S. Rietschel, *Natur Mus.* **98**, 409 (1968).
3. W. Stuermer, *ibid.*, p. 413.
4. F. Broili, *Neues Jahrb. Mineral. Geol. Palaeontol. Abt. B* **64**, 293 (1930).
5. W. M. Lehmann, *ibid.* **72**, 1 (1943).
6. W. Stuermer, *Paleontol. Z.* **43**, 10 (1969).
7. H. J. Harrington, "Eyes," in *Arthropoda 1* (part O of *Treatise on Invertebrate Paleontology*, R. C. Moore, Ed.) (Univ. of Kansas Press, Lawrence, 1959), p. O 87.
8. G. Lindström, *Kgl. Svenska Vetenskapsakad. Handl.* **34**, 1 (1901).
9. E. N. K. Clarkson, *Paleontology* **10**, 603 (1967).
10. ———, *Trans. Roy. Soc. Edinburgh* **68**, 183 (1969).
11. W. H. Miller, G. D. Bernard, J. L. Allen, *Science* **162**, 760 (1968).
12. F. Ratliff, H. K. Hartline, W. H. Miller, *J. Opt. Soc. Amer.* **53**, 110 (1963).
13. S. Exner, *Die Physiologie der facettirten Augen von Krebsen und Insecten* (Deuticke, Leipzig and Vienna, 1891).
14. I thank the Deutsche Forschungsgemeinschaft for support of part of this work.

27 April 1970

Hindered Diffusion in Microporous Membranes with Known Pore Geometry

Abstract. *The hindrance effect on the aqueous diffusion rate of solutes within membrane pores of molecular size has been accurately determined. Mica membranes, 3 to 5 micrometers thick, were prepared with uniform, straight pores from 90 to 600 angstroms in diameter. With these membranes a direct estimation was possible of the interaction between pore size and molecular diffusion rates. There were no uncertainties due to wide pore size distributions or nonuniform tortuous channels as in previously used model microporous materials such as dialysis tubing or gels. Aqueous diffusion rates through these mica membranes were measured for a series of compounds with molecular diameters from 5.2 to 43 angstroms and were corrected for "liquid film resistances" adjacent to the membrane-solution interface to obtain estimates of molecular diffusivities within the micropores of the membrane. Definite evidence is presented showing that, even when molecular size is a small fraction of pore size, diffusion rates decrease markedly. The apparent reduction in solute diffusivity in the microporous membrane can be quantitatively estimated by means of the Renkin equation for hindered diffusion.*

The extent of the influence of pore size on the liquid diffusion rate of solutes in microporous materials is important in biological membranes (*1*), separations by dialysis (*2*), and gel permeation chromatography (*3*). Although several investigators have attempted to quantitate the reduction in solute diffusivities within pores (*4*, *5*), the interpretation of the results obtained has been somewhat inconclusive in view of the fact that the porous ma-

terials used (gels, collodion filters, dialysis tubing) were of a rather inhomogeneous nature. The pores in these materials are really just the spaces in a polymeric brush pile structure, and the pore size distribution is unknown. Furthermore, the tortuousity is of necessity a function of molecular size and could not be independently characterized.

The work of Fleischer *et al.* (*6*) on the etching of fission particle tracks in mica suggested a means by which ideal membranes might be prepared in order to obtain more conclusive data on hindered diffusion. Fleischer *et al.* demonstrated that fission fragments from U^{235} would pass straight through thin sheets of mica, leaving behind tracks that could be etched with hydrofluoric acid to produce holes or pores in the mica film. By suitably spacing the U^{235} source from the mica film, the holes could be made almost perpendicular to the mica surface. Using this technique, Petzny and Quinn (*7*) demonstrated that the pore size could be systematically reduced with absorbed monomolecular layers; however, their work was limited to gas-phase diffusion.

Electron photomicrographs of membranes that were made by the process are shown in Fig. 1 (*8*). The hole size increases as the irradiated mica is etched for longer periods of time, and, when the holes become larger than 150 Å, they become diamond-like in cross section. Even though the shape of the pores changes with size, the pores are fairly uniform in size and can be characterized with respect to diffusion length and pore diameter. The tortuousity (diffusion path length divided by membrane thickness) of these membranes is approximately 1.01 (*9*), and there is no change in tortuousity with molecular size, as is the case with dialysis membranes. One of the primary experimental difficulties in this work was to prepare membranes with sufficient surface area and pore density, to give large enough solute transport rates, so that the relationship between pore size and the dimensions of permeant molecules in hindered diffusion could be accurately evaluated.

To insure that some of the etched fission tracks passed completely through the mica, the films had to be less than 8 μm in thickness. Pore density was estimated from electron photomicrographs of the membrane surface opposite to the entry point of the fission fragments. Membrane thickness was estimated by determining the density of the mica sheets and then weighing sheets of known surface area. After irradiation and etching the films were extremely brittle, and special holders had to be devised for the diffusion experiments; this fragility also made it necessary to design the diffusion apparatus so that the membranes were not subjected to pressure gradients greater than a few centimeters of water. These limitations on porosity (<5 percent) set the requirements for a closed recirculation diffusion apparatus with a small holdup volume (Fig. 2).

Table 1. Properties of probe molecules used in diffusion studies and typical permeability values for a microporous mica membrane.

Solute	Diffusion coefficient $\mathcal{D}_0$ at 25°C $\times 10^6$ (cm²/sec)	Molecular radius R_s (Å)	Membrane 48	
			Measured overall permeability $P_0 \times 10^4$ (cm/sec)	Corrected membrane permeability $P_m \times 10^4$ (cm/sec)
Urea	13.8	2.64 (*16*)	4.50	7.09
Glucose	6.73	4.44 (*16*)	2.40	3.42
Sucrose	5.21	5.55 (*16*)	1.80	2.45
Raffinose	4.34	6.54 (*16*)	1.46	1.92
2-Dextrin	3.44	8.00 (*2*)	1.06	1.33
β-Dextrin	3.22	8.98 (*2*)	0.95	1.17
Ribonuclease	1.18	21.6 (*17*)	0.090	0.093

We estimated pore diameters by determining water flow through the membrane at low pressure gradients and assuming Poiseuille's law to be valid for flow through the pores (*10*). The prepared mica membranes had equivalent pore diameters from 90 to 600 Å (see Fig. 3). Other independent estimates of pore diameters by gaseous flow and extrapolation of diffusion data (*8*) gave substantially the same values. A detailed study of electron photomicrographs for one membrane (membrane 48) showed a mean pore size of 133 Å with 85 percent of the pores having diameters from 110 to 150 Å. This pore size is in close agreement with estimates from the other methods and indicates the absence of large adsorbed films or immobilized layers of water inaccessible for solute diffusion along the interior pore walls.

In order to find the relationship between molecular diameter, pore size, and reduced diffusion rates in membranes, we measured the diffusion rates of a series of molecules with a wide range of molecular diameters from 5.2 to 43 Å (Table 1) through the series of mica membranes with different pore sizes. With the exception of ribonuclease, all of the compounds chosen in these experiments were nonelectrolytes so as to minimize electrical interactions with the mica membrane surface. The initial solute concentration difference across the membranes was about 0.05 percent by weight, and the gradient decreased as

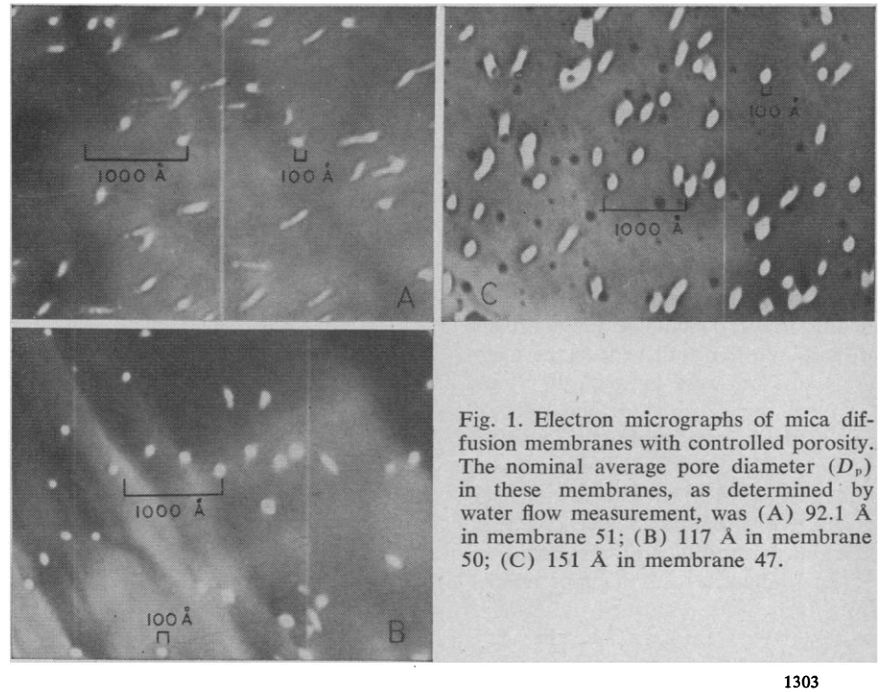

Fig. 1. Electron micrographs of mica diffusion membranes with controlled porosity. The nominal average pore diameter (D_p) in these membranes, as determined by water flow measurement, was (A) 92.1 Å in membrane 51; (B) 117 Å in membrane 50; (C) 151 Å in membrane 47.

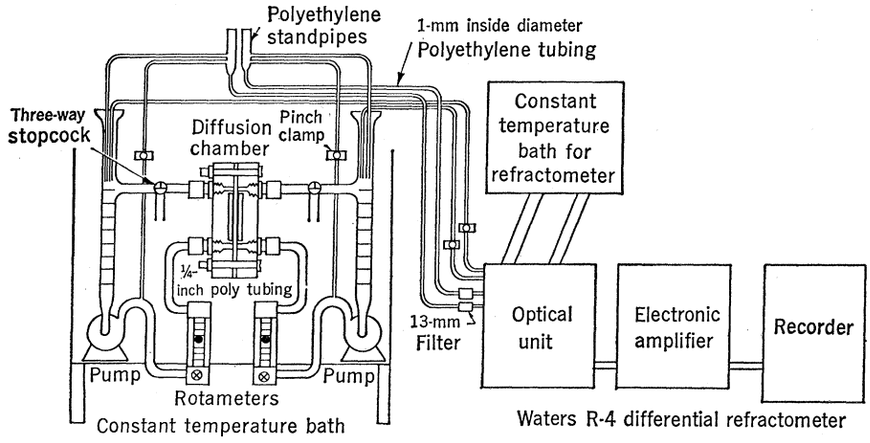

Fig. 2. Apparatus for diffusion measurements. Fluid is continuously recirculated past each side of the membrane. A portion of the fluid in each chamber is bypassed to a differential refractometer which continuously indicates the difference in solute concentration between the two chambers.

the experiment proceeded. Concentration changes were measured with a precision differential refractometer.

In determining the effective diffusivity of solutes in membranes it is of considerable importance to properly compensate for "stagnant films," "Nernst layers," or liquid film resistances adjacent to the membrane surface. The solute diffusion flux, J_s (in moles per square centimeter per second), is given by:

$$J_s = P_o \Delta C$$

where ΔC (in moles per cubic centimeter) is the overall concentration gradient of the solute and P_0 (in centimeters per second) is the overall permeability of the membrane and adjacent liquid resistances.

$$1/P_o = 1/P_m + 2/P_1$$

where P_m is the permeability of the membrane and P_1 is the permeability of the liquid resistances on each side of the membrane. Membrane permeability, P_m, is related primarily to solute size, whereas P_1 is also a function of the conditions of the liquid phase (velocity, density, viscosity) as well as of the solute diffusion coefficient (*11*).

The overall permeabilities of the membranes, P_0, including the resistance of the liquid films adjacent to the membrane surface, were between 10^{-3} and 10^{-4} cm/sec. Several methods, including electrochemical techniques and the use of calibrating membranes, were used to independently estimate the permeability of the liquid "layers," P_1. The effective permeability of the liquid resistances adjacent to the membrane surfaces alone were between 1.5×10^{-3} and 3×10^{-4} cm/sec (*12*). In many of the experiments the calculated concentration difference across the liquid film resistances was of the same order of magnitude as the concentration difference across the membrane itself. An illustration of the order of magnitude of the permeability corrections for the liquid phase resistance is given in Table 1 for membrane 48. The relative ratio of P_1 to P_m, and therefore the importance of correcting the data to estimate true membrane permeabilities, increases with smaller solutes and larger pore sizes.

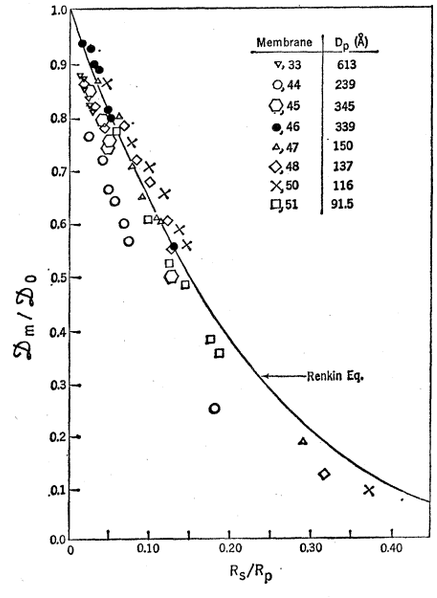

Fig. 3. Hindered diffusion in membrane pores as a function of the ratio of solute radius to pore radius (R_s/R_p). Membranes with pore diameters (D_p) from 91.5 to 613 Å were used in this study. The apparent diffusion coefficients of the solutes inside microporous channels, $\mathcal{D}_m$, were obtained from measured permeabilities and the known geometry of the pores (*10, 13*). The quantities $\mathcal{D}_0$ represent the free solution diffusivities of the same solutes (Table 1), and the ratio $\mathcal{D}_m/\mathcal{D}_0$ is a measure of the extent of hindrance within the pores.

The experimental design included diffusion measurements over the entire matrix of membrane pore sizes and molecular diameters, resulting in a rather complete coverage of the parameter R_s/R_p (ratio of solute radius to pore radius) which ranged from 0.01 to 0.38 over the many combinations tested. The measured overall permeabilities for the compounds were constant to within ± 2 percent during the experimental period of 2 to 6 hours, except for that of ribonuclease, which apparently increased about 30 percent during the course of a 20-hour period. Denaturation or adsorption may have occurred over this time period.

After the measured diffusion rates had been adjusted for the resistance of the liquid layers, the apparent diffusivity, $\mathcal{D}_m$, of the test molecules in the membrane pores was calculated (*13*). The ratio of this value to the diffusivity of the same compound in water ($\mathcal{D}_m/\mathcal{D}_0$) gives a measure of the hindrance effect of pores and is plotted against the ratio of molecular radius to pore radius in Fig. 3.

A rather striking reduction in solute diffusivity takes place within the micropore channels. For example, when the size ratio of solute to pore is 1/10, the mobility of the solute within the pore is almost 40 percent less than its mobility in free solution. At present, we do not have a detailed explanation for this huge interaction; however, the results can be correlated by means of an equation proposed by Renkin in 1954 (*5*):

$$\frac{\mathcal{D}_m}{\mathcal{D}_0} = \left(1 - \frac{R_s}{R_p}\right)^2 \times \left[1 - 2.10\left(\frac{R_s}{R_p}\right) + 2.09\left(\frac{R_s}{R_p}\right)^3 - 0.95\left(\frac{R_s}{R_p}\right)^5\right]$$

Here, the first term on the right-hand side is thought to represent an exclusion of solute from the membrane pores based on geometrical considerations and the second term represents an additional hydrodynamic drag on the solute molecules due to the proximity of the pore walls. On the basis of this equation, and in the range of solute to pore sizes (R_s/R_p) investigated here, about half the hindrance effect comes from molecular exclusion and the other half comes from viscous drag due to the wall.

The data in Fig. 3 are consistent with,

but do not prove the validity of, the Renkin equation for correlating the hindrance effect in microporous membranes. On the average, our data are about 4 percent below the values predicted by the Renkin equation. The data seem to be randomly scattered about the line, and there is no trend for the results for individual membranes, an indication that the correlation does not change with larger pores. The dimensionless ratio R_s/R_p seems to be a valid parameter for characterizing the hindrance effect over this range of pore sizes. Within the scatter of the experimental data, other empirical equations such as

$$\frac{\mathcal{D}_m}{\mathcal{D}_0} = \left(1 - \frac{R_s}{R_p}\right)^n$$

where n is about 4, correlate the data equally well.

Although the mechanism for the apparent drag on molecules as they pass through holes of molecular dimensions has not yet been determined, there can be no question that this effect does exist. In the experiments cited here, pore sizes were outside the range postulated for some natural membranes, such as the red blood cell, but within the range of pore sizes indicated for the kidney glomerulus (70 to 100 Å) (*14*). We have shown that the Renkin equation or similar correlations can be used with some confidence to evaluate pores in natural membranes (*15*).

On the basis of the data presented here, one can estimate the reduction in aqueous diffusion rates of solutes in porous materials, where the pores are of molecular dimensions, with a greater degree of confidence than has been possible heretofore. However, some knowledge of the structure of the porous material is required for such calculations, that is, average pore size, void fraction, and tortuousity. On the other hand, if the structure of the porous material is not well characterized, that is, if void fraction, pore size, or tortuousity is not known, then the use of diffusion studies with probe molecules and the correlation as presented in Fig. 3 can lead to information on the unknown parameter.

ROBERT E. BECK
JEROME S. SCHULTZ
Division of Chemical Engineering, University of Michigan, Ann Arbor

References and Notes

1. W. Ruhland and C. Hoffman, *Planta* **1**, 1 (1925); W. Wilbrandt, *Arch. Gesamte Physiol. Menschen Tiere (Pfluegers)* **241**, 302 (1938–39); J. W. Green, *J. Cell Comp. Physiol.* **33**, 247 (1949); J. R. Pappenheimer, E. M. Renkin, L. M. Borrero, *Amer. J. Physiol.* **167**, 13 (1951); J. R. Pappenheimer, *Physiol. Rev.* **33**, 307 (1953); C. V. Paganelli and A. K. Solomon, *J. Gen. Physiol.* **41**, 259 (1957); O. Giebel and H. Passow, *Arch. Gesamte Physiol. Menschen Tiere (Pfluegers)* **271**, 378 (1960).
2. L. C. Craig, *Science* **144**, 1093 (1964).
3. G. K. Akers, *Advan. Protein Chem.* **24**, 343 (1970).
4. E. Manegold, *Kolloid Z.* **49**, 372 (1929); J. D. Ferry, *J. Gen. Physiol.* **20**, 95 (1936); *Chem. Rev.* **18**, 373 (1936); H. Spandau and W. Gross, *Chem. Ber.* **74B**, 362 (1941); G. K. Akers and R. L. Steere, *Biochim. Biophys. Acta* **59**, 137 (1962); B. M. Uzelac and E. L. Cussler, *J. Colloid Interface Sci.* **32**, 487 (1970).
5. E. M. Renkin, *J. Gen. Physiol.* **38**, 225 (1954).
6. R. L. Fleischer, P. B. Price, R. M. Walker, *J. Appl. Phys.* **33**, 3407 (1962); *Rev. Sci. Instrum.* **34**, 510 (1963); R. L. Fleischer, P. B. Price, E. M. Symes, *Science* **143**, 249 (1964).
7. W. J. Petzny and J. A. Quinn, *Science* **166**, 751 (1969).
8. R. E. Beck, thesis, University of Michigan (1969).
9. The tortuousity is calculated from the average angle of incidence of the fission tracks with respect to the surface of the mica membrane. The fission foil was placed about 6 inches (15.2 cm) from the mica surface; the maximum angle of incidence of the fission fragments was about 15° from the normal, and the weighted average was about 8°.
10. Water flow through the membranes was measured under a 2-cm H_2O pressure gradient. Average pore radius was calculated from Poiseuille's law
$$R_p = \left(\frac{8QL\mu}{\pi NA\Delta p}\right)^{1/4}$$
where Q is the total water flow rate (in cubic centimeters per second), L is the membrane thickness, μ is the viscosity, N is the number of pores per unit membrane area, A is the area of the membrane, and Δp is the pressure gradient.
11. V. Levich, *Physicochemical Hydrodynamics* (Prentice-Hall, Englewood Cliffs, N.J., 1962).
12. Millipore (nominal pore diameter, 0.45 μm; membrane thickness, 25 μm; Millipore Co.) and Nucleopore (pore diameter, 0.8 μm; membrane thickness, 8 μm; General Electric Co.) membranes have large pores and therefore no restricted diffusion effects and relatively low diffusion resistance. The permeability (P_m) of these membranes was estimated from their physical properties, and subtracted from the overall diffusion resistance measured with each of the test solutes. The difference was attributed to liquid film resistances, that is,
$$P_l = 2/(P_o^{-1} - P_m^{-1})$$
Values for P_l were obtained for each of the test solutes in the diffusion cell under the same flow conditions as for the mica membranes. Estimates of the liquid film permeability (P_l) from measurements with these large pore membranes and from the electrochemical method agreed to within ± 5 percent.
13. Diffusion coefficients of solutes within the membrane pores were calculated by means of:
$$\mathcal{D}_m = \frac{P_m L}{\pi R_p^2 N}$$
14. D. A. Goldstein and A. K. Solomon, *J. Gen. Physiol.* **44**, 1 (1960); G. Wallenius, *Acta Soc. Med. Upsal. Suppl. 4* (1954); G. Giebisch, H. D. Lausen, R. F. Pitts, *Amer. J. Physiol.* **178**, 168 (1954).
15. A. K. Solomon, *J. Gen. Physiol.* (Suppl.) **51**, 335 (1968).
16. L. G. Longsworth, *J. Amer. Chem. Soc.* **75**, 5705 (1953).
17. F. J. Joubert and T. Haylett, *J. S. Afr. Chem. Inst.* **15**, 48 (1962).
18. Supported in part by PHS grant GM 15152.

12 May 1970; revised 24 July 1970 ■

Coral Skeletons: An Explanation of Their Growth and Structure

Abstract. *Coral skeletons are constructed of aragonitic crystals organized into fan systems. A theoretical model for the growth of such fan systems, which depends upon competition between crystals for space in which to grow, is corroborated by vital staining with sodium alizarinesulfonate. Fan systems of crystals compete with each other to form larger fan systems until large, relatively stable fans are produced. It is these relatively stable fan systems that have been observed in optical thin sections of coral skeletons.*

The microscopic appearance of coral skeletons is well known since it forms the basis of coral systematics (*1*). The basic unit of the skeleton is considered to be the sclerodermite, a group of fibers which fan out from a point called the center of calcification. Sclerodermites often grow vertically to produce a trabecula in which the fibers radiate outward and upward from a central axis which is supposed to be an elongated center of calcification. In most corals only the sclerosepta are trabecular. The sclerosepta comprise a palisade of trabeculae, each of which terminates in a dentation or tooth on the upper surface of the scleroseptum. Sorauf (*2*) and Wise (*3*) have shown that the fibers seen in optical section are acicular crystals, and both have confirmed that the crystals are normally organized into sclerodermites. They have shown that sclerodermites are fundamental to the structure of the dissepiments. I have found similar, though less organized, sclerodermites in the epitheca of three West Indian corals, and Wainwright (*4*) has described the development of sclerodermites on the basal plate of *Pocillopora damicornis*. Thus, all the parts of coral skeletons, so far examined, are built of crystals arranged in three-dimensional fans, and it seems appropriate to attempt to explain the development of these fans in terms of the physics of crystal growth.

I have followed the growth of sclerodermites and trabeculae by staining growing crystals red with sodium alizarinesulfonate, a dye used for vitally staining bone (*5*). When living corals and washed coral skeletons were placed in seawater containing about 20 mg of alizarine per liter, the washed skeletons were only stained on freshly damaged surfaces, whereas the skeletons of liv-